Applications and Applied Mathematics: An International Journal (AAM)

Volume 11 | Issue 2 Article 16

12-2016

Hydromagnetic peristaltic transportation with porous medium through an asymmetric vertical tapered channel and joule heating

S. R. Kumar
NBKR Institute of Science and Technology (Autonomous)

Available at
http://pvamu.edu/aam
Appl. Appl. Math.
ISSN: 1932-9466

Applications and Applied Mathematics:
An International Journal
(AAM)

Vol. 11, Issue 2 (December 2016), pp. 735 - 747

Hydromagnetic peristaltic transportation with porous medium through an asymmetric vertical tapered channel and joule heating

S. Ravi Kumar
Department of Mathematics
NBKR Institute of Science and Technology (Autonomous)
Vidyanagar, SPSR Nellore
Andhra Pradesh, India.Pin-524413
Email:drsravikumar1979@gmail.com;drsravikumar1979@nbkrist.org;

Received: February 2, 2016; Accepted: October 12, 2016

Abstract

The present paper deals with a theoretical investigation of the hydromagnetic peristaltic transportation with porous medium through coaxial asymmetric vertical tapered channel and joule heating which has been studied under the assumption of long wavelength approximations. Exact analytical expressions of axial velocity, volume flow rate, pressure gradient, temperature and heat transfer coefficient at both walls were calculated. The effects of various emerging parameters, Hartmann number, Non-uniform parameter, Prandtl number, Heat generator parameter, Brinkman number, Porous parameter are discussed through the use of graphs. We notice from the figures that the temperature of the fluid increases in the entire vertical tapered channel with an increase in Magnetic field, Brinkman number, Prandtl number and Heat generation parameter. We notice that the temperature profiles are found almost parabolic in nature. Further, it can be noticed that the heat transfer coefficient gradually decreases and then increases with increasing values of the Hartmann number, Brinkman number, Prandtl number, and Heat generation parameter in the entire vertical tapered channel at the right wall. It can be seen that the heat transfer coefficient slowly decreases and then increases in the rest of the channel with increasing values of the Hartmann number, Brinkman number, Prandtl number, and Heat generation parameter in entire vertical tapered channel at left the wall. It can be observed that the coefficient of heat transfer gives the oscillatory behaviour which is due to the propagation of peristaltic waves.

Keywords: Hartmann number; Porous medium; Tapered vertical channel; Joule heating

MSC 2010 No.: 76S05, 92B05, 74F10

1. Introduction

Peristalsis is now well known to physiologists to be one of the major mechanisms for fluid transport in many biological systems. Peristalsis is a natural mechanism of pumping that is observed in the case of most physiological fluids, which is generated by a progressive wave of contraction or expansion moving on the wall of the tube. The peristalsis mechanism is seen in many biological systems such as movement of chyme in the gastrointestinal tract, the transportation of urine from kidney to bladder, the ducts efferentes of the male reproductive tract, swallowing of food through esophagus, blood circulation in the small blood vessels, movement of ovum in the female fallopian tube, transport of cilia, vasomotion of small blood vessels such as arterioles, the locomotion of some worms, transport of lymph in the lymphatic vessels, venules and capillaries and transport of bile in the bile duct.

Recently, peristaltic fluid flows in asymmetric channel have gained the attention of researchers working in this field. Also, the peristaltic phenomenon is used in many industrial applications like sanitary fluids, blood pumps in heart-lung machines, and transport of corrosive fluids. There are many other applications of peristalsis such as the design of roller pumps, which are useful in pumping fluids without contamination due to contact with the pumping machinery. LATHAM (1968) made initial attempts regarding peristaltic mechanism of viscous fluid. Initial mathematical models of peristalsis obtained by a train of sinusoidal waves in an infinitely long symmetric channel or tube were introduced by Fung and Yih (1969) and Shapiro et al. (1977).

After these studies, several analytical, numerical, and experimental attempts have been made to understand peristaltic action in different situations for Newtonian and non-Newtonian fluids. Some of these studies have been done by (Takabatake and Ayukawa (1982), Takabatake and Ayukawa (1988), Srivastava (1986), Srivastava and Srivastava (1984), Srivastava and Srivastava (1988), Srivastava et al. (1983), Siddiqui and Schwarz (1994), Ramachandra and Usha (1995), Elshehawey and Sobh (2001), Elbarbary (2000), Sobh (2004), Abd El Naby et al. (2004), Hayat et al. (2007), Ravikumar et al. (2010), Ravikumar and Siva Prasad (2010), Ravikumar (2013), Ravikumar et al. (2010), Ravikumar (2013), Ravikumar (2015), Ravikumar (2014), Ravikumar (2015), Ravikumar (2013)). Heat transfer is the transition of thermal energy from a region of higher temperature to a region of lower temperature.

The transfer of thermal energy continues until the object and its surroundings reach the state of thermal equilibrium. The energy transfer by heat flow cannot be measured directly. However, the concept has physical meaning because it is related to the measurable quantity called temperature. Once the temperature difference is known, a quantity of practical interest, the heat flux which is the amount of heat transfer per unit time is readily determined. Heat transfer on the peristaltic mechanism is also important in many physiological applications as well as engineering. This mechanism may occur in obtaining information about properties of hypothermia treatment, blood pump in heart-lung machines, tissues, sanitary fluid transport and transport of corrosive fluids Nadeem and Akram (2011). Some more work on this topic can be seen in (Nadeem and Akbar (2008), Vajravelu et al. (2011), Srinivas and Kothandapani (2008), Seddeek and Almushigeh (2010), Hayat et al. (2014), Oahimire and Olajuwon (2014), Mehmood et al. (2012), Sengupta (2015), Saleem and Haider (2014), Tripathi and Beg (2014), and Radhakrishnamacharya and Srinisvasulu (2007).)

2. Mathematical formulation

Let us consider the peristaltic flow of an incompressible viscous fluid with porous medium through a coaxial vertical asymmetric tapered channel under the action of a magnetic field. Asymmetry in the flow is due to the propagation of peristaltic waves of different amplitudes and phase on the channel walls. The heat transfer in the channel is taken into account. The flow is generated by sinusoidal wave trains propagating with constant speed c along the tapered asymmetric channel walls

$$Y = H_2 = b + m'X + d\sin\left[\frac{2\pi}{\lambda}(X - ct)\right], \tag{1a}$$

$$Y = H_1 = -b - m'X - d\sin\left[\frac{2\pi}{\lambda}(X - ct) + \phi\right], \tag{1b}$$

where b is the half-width of the channel, d is the wave amplitude, c is the phase speed of the wave and $m^I (m^I << 1)$ is the non-uniform parameter, λ is the wavelength, t is the time and X is the direction of wave propagation. The phase difference ϕ varies in the range $0 \le \phi \le \pi$, $\phi = 0$ corresponds to symmetric channel with waves out of phase and further b, d and ϕ satisfy the following conditions for the divergent channel at the inlet $d\cos(\frac{\phi}{2}) \le b$.

It is assumed that the left wall of the channel is maintained at temperature T_0, while the right wall has temperature T_1.

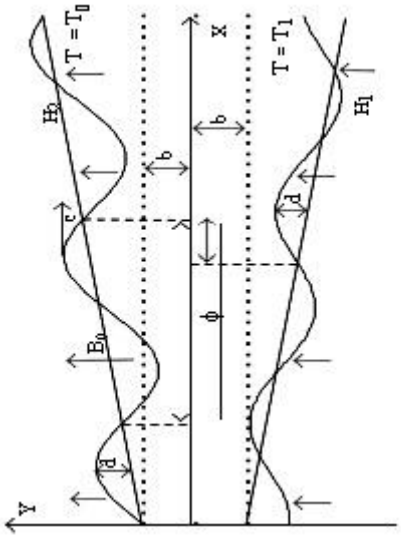

Figure 1. Schematic diagram of the physical model

The equations governing the motion for the present problem are

$$\frac{\partial u}{\partial x}+\frac{\partial v}{\partial y}=0, \tag{2}$$

$$\rho\left[\frac{\partial u}{\partial t}+u\frac{\partial u}{\partial x}+v\frac{\partial u}{\partial y}\right]=-\frac{\partial p}{\partial x}+\mu\left[\frac{\partial^2 u}{\partial x^2}+\frac{\partial^2 u}{\partial y^2}\right]-\left[\sigma B_0{}^2\right](u+c)-\left[\frac{\mu}{k_1}\right](u+c)+g\sin\alpha, \tag{3}$$

$$\rho\left[\frac{\partial u}{\partial t}+u\frac{\partial v}{\partial x}+v\frac{\partial v}{\partial y}\right]=-\frac{\partial p}{\partial y}+\mu\left[\frac{\partial^2 v}{\partial x^2}+\frac{\partial^2 v}{\partial y^2}\right]-\left[\sigma B_0{}^2\right]v-\left[\frac{\mu}{k_1}\right]v-g\cos\alpha, \tag{4}$$

$$\rho C_p\left[\frac{\partial}{\partial t}+u\frac{\partial}{\partial x}+v\frac{\partial}{\partial y}\right]T=k\left[\frac{\partial^2}{\partial x^2}+\frac{\partial^2}{\partial y^2}\right]T+Q_0+\sigma B_0{}^2u^2, \tag{5}$$

u and v are the velocity components in the corresponding coordinates, p is the fluid pressure ρ is the density of the fluid, μ is the coefficient of the viscosity, k_1 is the permeability of the porous medium and k is the thermal conductivity, C_p is the specific heat at constant pressure, Q_0 is the constant heat addition/absorption and T is the temperature of the fluid.

Introducing a wave frame (x, y) moving with velocity c away from the fixed frame (X, Y), the transformations

$$x = X\text{-}ct,\ y = Y,\ u = U\text{-}c,\ v = V \text{ and } p(x) = P(X, t), \tag{6}$$

where u, v are the velocities in the x and y directions in the wave frame and p is the pressure in wave frame.

Introducing the following non-dimensional quantities:

$$\left.\begin{aligned}&\overline{x}=\tfrac{x}{\lambda},\overline{y}=\tfrac{y}{b},\overline{u}=\tfrac{u}{c},\overline{v}=\tfrac{v}{c},h_1=\tfrac{H_1}{b},h_2=\tfrac{H_2}{b},p=\tfrac{b^2p}{c\lambda\mu},Da=\tfrac{k_1}{b^2},\theta=\tfrac{T-T_0}{T_1-T_0},\\&\epsilon=\tfrac{d}{b},\Pr=\tfrac{\mu C_p}{k},E_c=\tfrac{c^2}{C_p(T_1-T_0)},\delta=\tfrac{b}{\lambda},Re=\tfrac{\rho c b}{\mu},M=B_0b\sqrt{\tfrac{\sigma}{u}},\beta=\tfrac{Q_0b^2}{\mu C_p(T_1-T_0)},\end{aligned}\right\} \tag{7}$$

where $\varepsilon=\frac{d}{b}$ is the non-dimensional amplitude of channel, $\delta=\frac{b}{\lambda}$ is the wave number $k_1=\frac{\lambda m'}{b}$ is the non - uniform parameter, *Da* is the porous parameter, *Re* is the Reynolds number, *M* is the Hartmann number, $K=\frac{k}{b^2}$. Permeability parameter, Pr is the Prandtl number β is the heat generation parameter, *Br* is the Brinkman number and E_c is the Eckert number.

3. Solution of the problem

In view of the above transformations (6) and non-dimensional variables (7), Equations (2-5) are reduced to the following non-dimensional form after dropping the bars.

$$\mathrm{Re}\,\delta\left[\frac{\partial u}{\partial t}+u\frac{\partial u}{\partial x}+v\frac{\partial u}{\partial y}\right]$$

$$=\left[-\frac{\partial p}{\partial x}+\delta^2\frac{\partial^2 u}{\partial x^2}+\frac{\partial^2 u}{\partial y^2}-\left(M^2+\frac{1}{Da}\right)u-\left(M^2+\frac{1}{Da}\right)+\eta\sin\alpha\right], \tag{8}$$

$$\mathrm{Re}\,\delta^3\left[\frac{\partial v}{\partial t}+u\frac{\partial v}{\partial x}+v\frac{\partial v}{\partial y}\right]$$

$$=\left[-\frac{\partial p}{\partial y}+\delta^4\frac{\partial^2 v}{\partial x^2}+\delta^2\frac{\partial^2 v}{\partial y^2}-M^2\delta^2 v-\frac{1}{Da}v-\eta_1\cos\alpha\right], \tag{9}$$

$$\mathrm{Re}\left[\delta\frac{\partial\theta}{\partial t}+\delta u\frac{\partial\theta}{\partial x}+v\frac{\partial\theta}{\partial y}\right]=\frac{1}{\mathrm{Pr}}\left[\delta^2\frac{\partial^2\theta}{\partial x^2}+\frac{\partial^2\theta}{\partial y^2}\right]+\beta+M^2E_c\,u^2. \tag{10}$$

Applying long wave length approximation and neglecting the wave number along with low-Reynolds numbers Equations (9 -11) become

$$\frac{\partial^2 u}{\partial y^2}-\left(M^2+\frac{1}{D}\right)u=\frac{\partial p}{\partial x}+\left(M^2+\frac{1}{D}\right)-\eta\sin\alpha, \tag{11}$$

$$\frac{\partial p}{\partial y}=0, \tag{12}$$

$$\frac{1}{\mathrm{Pr}}\left(\frac{\partial^2\theta}{\partial y^2}\right)+\beta+B_r\,u^2=0. \tag{13}$$

The corresponding boundary conditions in dimensionless form are given by

$$u = -1,\ \theta = 0 \text{ at } \quad y=h_1=-1-k_1x-\varepsilon\sin\left[2\pi(x-t)+\phi\right], \tag{14a}$$

$$u = -1,\ \theta = 1 \text{ at } y=h_2=1+k_1x+\varepsilon\sin\left[2\pi(x-t)\right]. \tag{14b}$$

The closed form solutions for Equations (11-13) with boundary conditions (14a) and (14b) are

$$u=a_1\,Sin\,h[\alpha_1 y]+a_2\,Cos\,h\,[\alpha_1 y]+A, \tag{15}$$

where

$$a_1=\left[\frac{-(1+A)}{Sinh(\alpha_1h_1)}\right]\left[1+\left[\frac{Cosh(\alpha_1h_2)}{\left[\frac{Cosh(\alpha_1h_1)-Cosh(\alpha_1h_2)}{Sinh(\alpha_1h_1)-Sinh(\alpha_1h_2)}\right]Sinh(\alpha_1h_1)-Cosh(\alpha_1h_1)}\right]\right],$$

$$a_2 = \left(\frac{(1+A)}{\left[\frac{Cosh(\alpha_1 h_1) - Cosh(\alpha_1 h_2)}{Sinh(\alpha_1 h_1) - Sinh(\alpha_1 h_2)} \right] Sinh(\alpha_1 h_1) - Cosh(\alpha_1 h_1)} \right),$$

$$A = \frac{D}{M^2 D+1} \left(\eta \sin\alpha - \frac{\partial p}{\partial x} \right) - 1,$$

$$\theta = H + Gy - \beta \Pr \frac{y^2}{2} - M^2 B_r \left[\frac{y^2}{4} \left(2A^2 - a_1^{\,2} + a_2^{\,2} \right) + \frac{2Aa_1 Sinh(\alpha_1 y)}{\alpha_1^{\,2}} + \frac{2Aa_2 Cosh(\alpha_1 y)}{\alpha_1^{\,2}} \right]$$

$$- M^2 B_r \left[\frac{a_1 a_2 Sinh(2\alpha_1 y)}{4\alpha_1^{\,2}} + \frac{\left(a_1^{\,2} + a_2^{\,2} \right) Cosh(2\alpha_1 y)}{8\alpha_1^{\,2}} \right], \tag{16}$$

where

$$H = 1 - Gh_2 + \beta P_r \frac{h_2^{\,2}}{2} + M^2 B_r \frac{h_2^{\,2}}{4} \left[2A^2 - a_1^{\,2} + a_2^{\,2} \right] + \left(M^2 B_r \frac{2Aa_1 \sinh(\alpha_1 h_2)}{a_1^{\,2}} \right)$$

$$+ \left(\frac{(a_1^{\,2} + a_2^{\,2}) \cosh(2\alpha_1 h_2) a_1 a_2}{8\alpha_1^{\,2}} \right) + \left(M^2 B_r \frac{2Aa_2 \cosh(\alpha_1 h_2)}{\alpha_1^{\,2}} \right) + \left(M^2 B_r \frac{\sinh(\alpha_1 h_2) a_1 a_2}{4\alpha_1^{\,2}} \right),$$

$$G = \left(\frac{-1}{(h_1 - h_2)} \right) \left(1 + \beta P_r \left(\frac{h_2^{\,2}}{2} - \frac{h_1^{\,2}}{2} \right) + M^2 B_r \left(\frac{h_2^{\,2}}{4} - \frac{h_1^{\,2}}{4} \right) \left(2A^2 - a_1^{\,2} + a_2^{\,2} \right) \right.$$

$$+ \left(M^2 B_r \frac{2\,\mathrm{A}\,\mathrm{a}_1 \left[\sinh(\alpha_1 h_2) - \sinh(\alpha_1 h_1) \right]}{\alpha_1^{\,2}} \right)$$

$$+ \left(M^2 B_r \frac{2\,\mathrm{A}\,\mathrm{a}_2 \left[\cosh(\alpha_1 h_2) - \cosh(\alpha_1 h_1) \right]}{\alpha_1^{\,2}} \right)$$

$$\left. + \left(M^2 B_r \frac{\mathrm{a}_1\,\mathrm{a}_2 \left[\sinh(2\alpha_1 h_2) - \sinh(2\alpha_1 h_1) \right]}{4\alpha_1^{\,2}} \right) \right),$$

$$+ \left(M^2 B_r \frac{(a_1^{\,2} + a_2^{\,2}) \left[\cosh(2\alpha_1 h_2) - \cosh(2\alpha_1 h_1) \right]}{8\alpha_1^{\,2}} \right).$$

The coefficients of the heat transfer Zh_1 and Zh_2 at the walls $y = h_1$ and $y = h_2$ respectively, are given by

$$Zh_1 = \theta_y h_{1x}. \tag{17}$$

$$Zh_2 = \theta_y h_{2x}. \tag{18}$$

The solutions of the Equations (17) and (18) are

$$Zh_1 = \theta_y h_{1x} = \left(G - \beta \Pr y - M^2 B_r \left[\left(\frac{y}{2}(2A^2 - {a_1}^2 + {a_2}^2)\right) + \frac{2Aa_1 \cos h(\alpha_1 y)}{\alpha_1} + \frac{2Aa_2 \sin h(\alpha_1 y)}{\alpha_1}\right] - M^2 B_r \left(\frac{a_1 a_2 \cosh(2\alpha_1 y)}{2\alpha_1}\right) + \left(\frac{({a_1}^2 + {a_2}^2)\sinh(2\alpha_1 y)}{4\alpha_1}\right)\right) * (-2\pi\epsilon \cos[2\pi(x-t) + \phi] - k_1). \quad (19)$$

$$Zh_2 = \theta_y h_{2x} = \left(G - \beta \Pr y - M^2 B_r \left[\left(\frac{y}{2}(2A^2 - {a_1}^2 + {a_2}^2)\right) + \frac{2Aa_1 \cos h(\alpha_1 y)}{\alpha_1} + \frac{2Aa_2 \sin h(\alpha_1 y)}{\alpha_1}\right] - M^2 B_r \left(\frac{a_1 a_2 \cosh(2\alpha_1 y)}{2\alpha_1}\right) + \left(\frac{({a_1}^2 + {a_2}^2)\sinh(2\alpha_1 y)}{4\alpha_1}\right)\right) * (2\pi\epsilon \cos[2\pi(x-t)] - k_1). \quad (20)$$

4. Volumetric flow rate

The rate of volume flow q through each section is a constant (independent of both x and t). It is given by

$$q = \int_{h_1}^{h_2} u\, dy = \int_{h_1}^{h_2} \left(a_1 Sin[\alpha_1 y] + a_2 Cos[\alpha_1 y] + A\right) dy = -a_5 + a_6 + A\left[\left(h_2 - h_1\right) - a_5 + a_6\right], \quad (21)$$

where

$$a_5 = \left[\frac{-\left(Cosh(\alpha_1 h_2) - Cosh(\alpha_1 h_1)\right)}{\alpha_1 Sinh(\alpha_1 h_1)}\right]\left[1 + \left[\frac{Cosh(\alpha_1 h_2)}{\left[\frac{Cosh(\alpha_1 h_1) - Cosh(\alpha_1 h_2)}{Sinh(\alpha_1 h_1) - Sinh(\alpha_1 h_2)}\right] Sinh(\alpha_1 h_1) - Cosh(\alpha_1 h_1)}\right]\right],$$

$$a_6 = \frac{1}{\alpha_1}\left[\frac{(Sinh(\alpha_1 h_2) - Sinh(\alpha_1 h_1))}{\left(\left(\frac{Cosh(\alpha_1 h_1) - Cosh(\alpha_1 h_2)}{Sinh(\alpha_1 h_1) - Sinh(\alpha_1 h_2)}\right) Sinh(\alpha_1 h_1)\right) - Cosh(\alpha_1 h_1)}\right],$$

Hence, the flux at any axial station in the fixed frame is found to be

$$Q = \int_{h_2}^{h_1} (u + 1)\, dy = q + (h_1 - h_2). \quad (22)$$

The average volume flow rate over one wave period ($T = \lambda/c$) of the peristaltic wave is defined as

$$\overline{Q} = \frac{1}{T}\int_0^T Q dt = \frac{1}{T}\int \left(q + (h_1 - h_2)\right) dy = q + 1 + d\,. \quad (23)$$

The pressure gradient obtained from Equation (15) can be expressed as

$$\frac{dp}{dx} = (\eta \sin\alpha) - \left(\frac{\left(\overline{Q} - (1+d)\right) - (a_6 - a_5)}{(h_1 - h_2) + (a_6 - a_5)} \right) \left(M^2 + \frac{1}{D} \right) - \left(M^2 + \frac{1}{D} \right). \quad (24)$$

The pressure rise Δ_P (at the wall) in the channel of length L, non-dimensional form is given by

$$\Delta p = \int_0^1 \left(\frac{dp}{dx} \right) dx = \int_0^1 \left((\eta \sin\alpha) - \left(\frac{\left(\overline{Q} - (1+d)\right) - (a_6 - a_5)}{(h_1 - h_2) + (a_6 - a_5)} \right) \right) \left(M^2 + \frac{1}{D} \right) - \left(M^2 + \frac{1}{D} \right) dx \ .$$

5. Numerical results and discussion

The primary object of this investigation has been to study Hydromagnetic peristaltic transportation with porous medium through coaxial asymmetric vertical tapered channel and joule heating point, The analytical expressions for velocity distribution, pressure gradient, temperature and heat transfer coefficient have been derived in the previous section. The numerical and computational results are discussed through the graphical illustration. **Mathematica** software is used to find out numerical results.

Figure 2(a) presents the flow structure of the temperature (θ) for different values of Hartmann number (M = 1, 2, 3) with β = 0.5, B_r = 0.1, P_r = 1, Da = 0.1, η = 0.5, P = -0.5, k_1= 0.1, x = 0.6, t = 0.4, ε = 0.2, $\phi = \pi/6$, $\alpha = \pi/6$. Indeed, the temperature of the fluid increases with increasing values of Hartmann number. Figure 2(b) depicts the temperature profile for different values of B_r (B_r = 0.1, 0.3, 0.5) with β = 0.5, M = 1, P_r = 1, Da = 0.1, η = 0.5, P = -0.5, k_1= 0.1, x = 0.6, t = 0. 4, ε = 0.2, $\phi = \pi/6$, $\alpha = \pi/6$. It can be seen from the figure that the temperature of the fluid increases with increasing values of B_r. We conclude that the temperature of the fluid increases with increasing values of M and B_r.

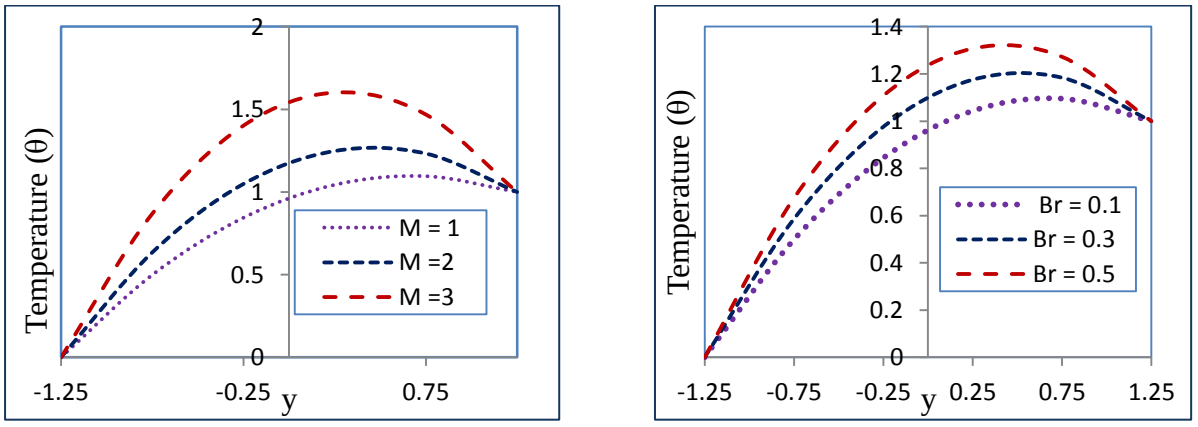

2(a) 2(b)

Figure 2. Temperature (θ) profile for different values of M and B_r

Figure 3(a) shows that the temperature (θ) profile for different values of Prandtl number (P_r = 1, 1.25, 1.5) with β = 0.5, B_r = 0.1, M = 1, Da = 0.1, η = 0.5, P = -0.5, k_1= 0.1, x = 0.6, t = 0.4, ε = 0.2, $\phi = \pi/6$, $\alpha = \pi/6$. Indeed, the temperature of the fluid increases with increasing values of Prandtl number (Pr). Figure 3(b) depicts the temperature profile for different values of β (β = 0.5, 0.7, 0.9) with P_r = 1, B_r = 0.3, M = 1, Da = 0.1, η = 0.5, P = -0.5, k_1= 0.1, x = 0.6, t = 0.4, ε = 0.2, $\phi = \pi/6$, $\alpha = \pi/6$. It was observed that the temperature of the fluid increases with increasing values of β. Finally, we notice that the temperature of the

fluid increases with increasing values of M, B_r, P_r and β in the entire vertical tapered channel (Figures 2 and 3).

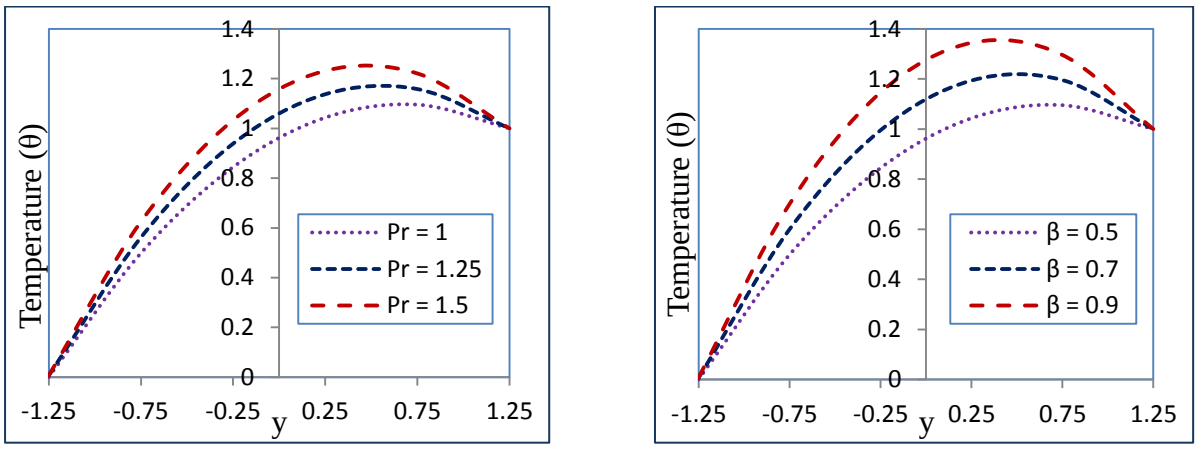

3(a) 3(b)

Figure 3. Temperature (θ) profile for different values of Pr and β

Figure 4(a) illustrates the flow structure of heat transfer coefficient at the wall $y = h_1$ for different values of M (M = 1, 2, 3) with B_r = 0.1, β = 0.5, P_r = 1, Da = 0.1, η = 0.5, P = -0.5, k_1= 0.1, t = 0.4, ε = 0.2, $\phi = \pi/4$, $\alpha = \pi/6$. We notice that heat transfer coefficient decreases in the portion of the channel $x \in [0, 0.6]$ and then increases in the range $x \in [0.6, 1]$ with increasing values of Hartmann number. In Figure 4(b), the effects of Brinkman number Br (B_r = 0.1, 0.3, 0.5) on heat transfer coefficient at the wall $y = h_1$ with fixed P_r = 1, β = 0.5, M = 1, Da = 0.1, η = 0.5, P = -0.5, k_1= 0.1, t = 0.4, ε = 0.2, $\phi = \pi/4$, $\alpha = \pi/6$ is illustrated. Inspection of this figure indicates that the heat transfer coefficient decreases in the portion of the channel $x \in [0, 0.6]$ and then increases in the rest of the channel $x \in [0.6, 1]$ with increasing values of B_r.

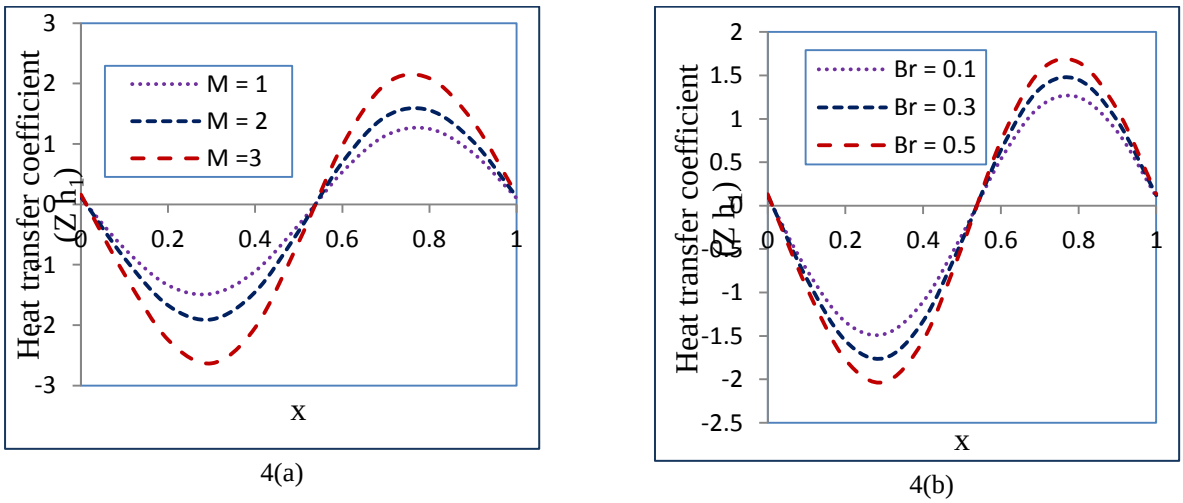

4(a) 4(b)

Figure 4. Heat transfer coefficient at the wall $y = h_1$ for different values of M and B_r

Figure 5(a) displays the impact of Prandtl number P_r (P_r = 1, 1.25, 1.5) on heat transfer coefficient at the wall $y = h_1$ with B_r = 0.1, β = 0.5, M = 1, Da = 0.1, η = 0.5, P = -0.5, k_1= 0.1, t = 0. 4, ε = 0.2, $\phi = \pi/4$, $\alpha = \pi/6$. We notice that heat transfer coefficient decreases in the portion of the channel $x \in [0, 0.6]$ and then increases in the rest of channel $x \in [0.6, 1]$ with increasing values of Prandtl number (Pr). Figure 5(b) shows that the flow structure of

heat transfer coefficient at the wall $y = h_1$ for different values of heat generation parameter β (β = 0.5 0.7, 0.9) with fixed $B_r = 0.1$, $M = 1$, $P_r = 1$, $Da = 0.1$, η = 0.5, $P = -0.5$, $k_1 = 0.1$, $t = 0.4$, ε = 0.2, $\phi = \pi/4$, $\alpha = \pi/6$. It can be noticed that heat transfer coefficient decreases in the range $x \in [0, 0.6]$ and then it is increases in the other portion of the channel $x \in [0.6, 1]$ with higher values of β.

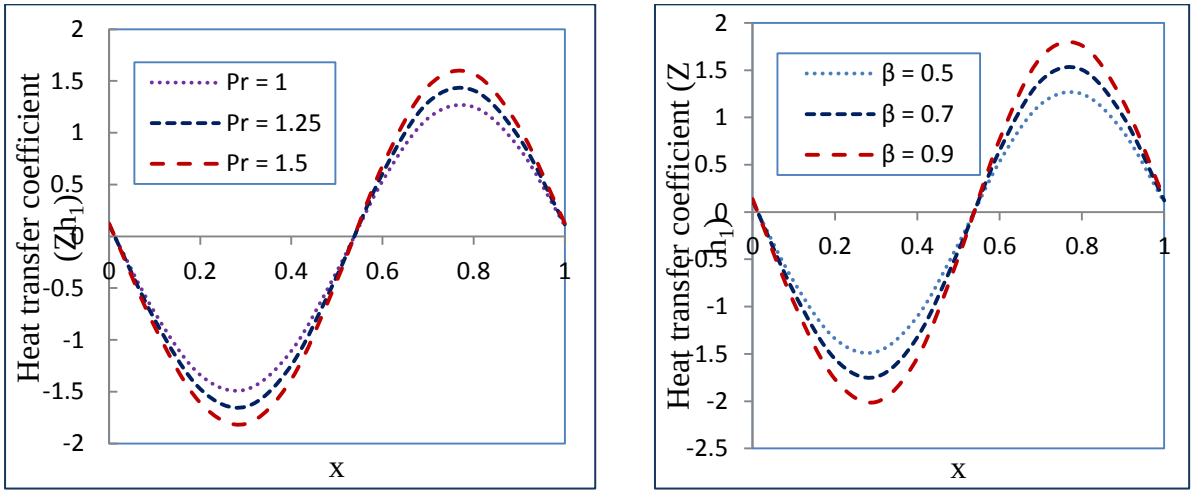

5(a) 5(b)

Figure 5. Heat transfer coefficient at the wall $y = h_1$ for different values of Pr and β

Figure 6(a) shows that the heat transfer coefficient at the wall $y = h_2$ for different values of M (M = 1, 2, 3) with $B_r = 0.1$, β = 0.5, $P_r = 1$, $Da = 0.1$, η = 0.5, $P = -0.5$, $k_1 = 0.1$, $t = 0.4$, ε = 0.2, $\phi = \pi/4$, $\alpha = \pi/6$. We notice that heat transfer coefficient decreases in the portion of the channel $x \in [0.1, 0.7]$ and then increases in the rest of the channel $x \in [0, 0.1] \cup [0.7,1]$ with increasing values of Hartmann number. Figure 6(b) presents the flow structure of heat transfer coefficient at the wall $y = h_2$ for different values of Br (B_r = 0.1, 0.3, 0.5) with fixed $P_r = 1$, β = 0.5, $M = 1$, $Da = 0.1$, η = 0.5, $P = -0.5$, $k_1 = 0.1$, $t = 0.4$, ε = 0.2, $\phi = \pi/4$, $\alpha = \pi/6$. It can be observed from this figure that heat transfer coefficient decreases in the channel $x \in [0.1, 0.7]$ and then increases in the other range $x \in [0, 0.1] \cup [0.7,1]$ with increasing values of B_r.

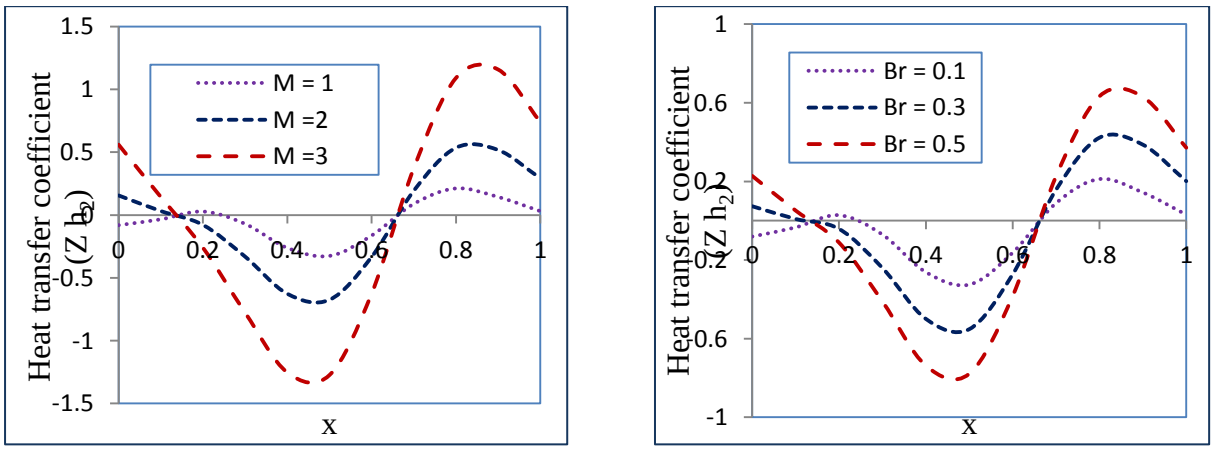

6(a) 6(b)

Figure 6. Heat transfer coefficient at the wall $y = h_2$ for different values of M and B_r

The effect of Prandtl number (P_r = 1, 1.25, 1.5) on heat transfer coefficient at the wall $y = h_2$ with $B_r = 0.1$, β = 0.5, M = 1, $Da = 0.1$, η = 0.5, $P = -0.5$, $k_1 = 0.1$, $t = 0.4$, ε = 0.2, $\phi = \pi/4$,

$\alpha = \pi/6$ is illustrated in Figure 7(a). We notice from the figure that the heat transfer coefficient decreases in the channel $x \in [0.1, 0.7]$ and then increases in the range $x \in [0, 0.1] \cup [0.7,1]$ with increasing values of Prandtl number. Figure 7(b) represents the flow structure of heat transfer coefficient at the wall $y = h_2$ for different values of β (β = 0.5 0.7, 0.9) with fixed Br = 0.1, M = 1, P_r = 1, Da = 0.1, η = 0.5, P = -0.5, k_1= 0.1, t = 0.4, ε = 0.2, $\phi = \pi/4$, $\alpha = \pi/6$. We notice that heat transfer coefficient decreases in the range $x \in [0.1, 0.7]$ and then increases in the rest of the channel $x \in [0, 0.1] \cup [0.7,1]$ with increasing values of β. Further, it can be noticed in all the Figures 4-7, the coefficient of heat transfer gives the oscillatory behaviour, which is due to the propagation of peristaltic waves.

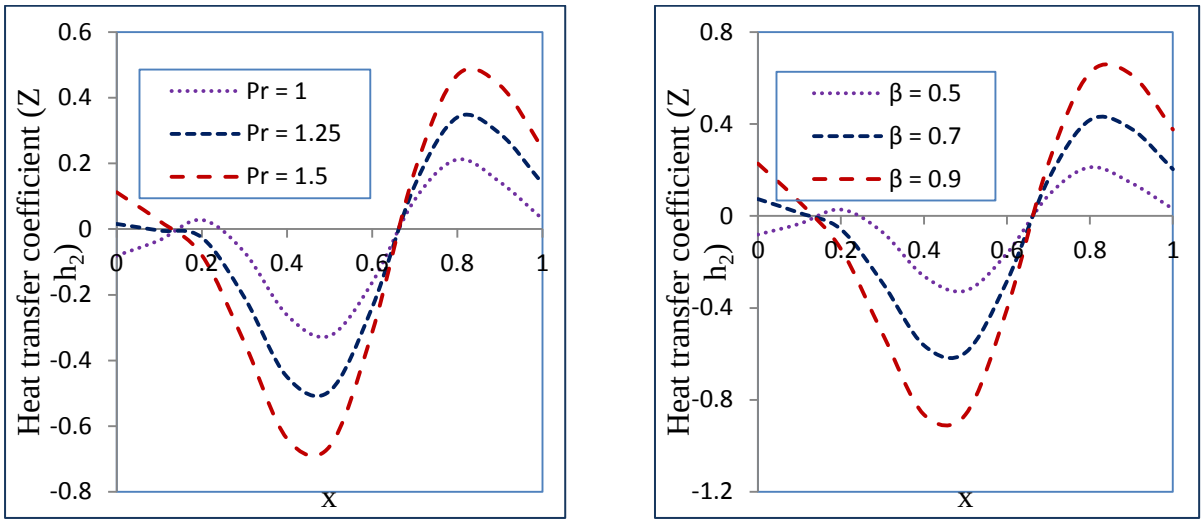

7(a) 7(b)

Figure 7. Heat transfer coefficient at the wall $y = h_2$ for different values of Pr and β

6. Conclusion

Hydromagnetic peristaltic transportation with porous medium through coaxial asymmetric vertical tapered channel and joule heating is investigated under the assumption of long wavelength approximation. We conclude with the following observations:

1. The temperature of the fluid increases in the entire tapered vertical channel with increasing values of M, B_r, P_r and β.
2. Heat transfer coefficient at the wall $y = h_1$ decreases in the portion of the channel $x \in [0, 0.6]$ and then increases in the other portion of the channel $x \in [0.6, 1]$ with increasing values of M, Br, Pr and β.
3. Heat transfer coefficient at the wall $y = h_2$ decreases in the portion of the channel $x \in [0.1, 0.7]$ and then increases in the channel $x \in [0, 0.1] \cup [0.7, 1]$ with increasing the values of M, Br, Pr and β.

Acknowledgement:

We would like to thank the reviewers and editors for their encouraging comments and constructive suggestions in improving the manuscript of the present study.

REFERENCES

Abd El Naby, A. H., El Misery, A.M. and Abd El Kareem, M. (2004). Separation in the flow through Peristaltic Motion of a Carreau Fluid in Uniform Tube. Physica A: Statistical mechanics and its application, 343, 1-14.

Brown, T. D. and Hung, T.K. (1977). Computational and Experimental Investigations of Two-Dimensional Non-Linear Peristaltic Flows. Journal of Fluid Mechanics, 83, 249-273.

Dharmendra Tripathi and Anwar Beg, O. (2014). A study on peristaltic flow of Nanofluids: Application in drug delivery, systems. International Journal of Heat and Mass Transfer, 70, 61-70.

Elbarbary, E.M. (2000). Peristaltic motion of a generalized Newtonian fluid through a porous medium. J. of Physical Society of Japan, 69, 401-407.

Elshehawey, Efland Sobh, A.M. (2001). Peristaltic Viscoelastic Fluid Motion in a Tube. International Journal of Mathematics and Mathematical Sciences, 26, 21- 34.

Fung, Y.C. and Yih, C.S. (1968). Peristaltic Transport. J. Appl. Mech. 35, 669-675.

Hayat, T., Ambreen, A., Khan, M. and Asghar, S. (2007). Peristaltic Transport of a Third Order Fluid under the Effect of a Magnetic Field. Computers and Mathematics with Applications, 53, 1074-1087.

Hayat, T., Humaira Yasmina and Maryem Al- Yam. (2014). Soret and Dufour effects in peristaltic transport of physiological fluids with chemical reaction: A mathematical analysis. Computers and Fluids, 89, 242- 253.

Mehmood, O, U., Mustapha, N. and Shafie, S. (2012). Heat transfer on peristaltic flow of fourth grade fluid in inclined asymmetric channel with partial slip. Appl. Math. Mech. -Engl. Ed., 33(10), 1313-1328.

Musharafa Saleem and Aun Haider. (2014). Heat and mass transfer on the peristaltic transport of non-Newtonian fluid with creeping flow. International Journal of Heat and Mass Transfer, 68, 514-526.

Nadeem, S. and Noreen Sher Akbar. (2008). Effects of heat transfer on the peristaltic transport of MHD Newtonian fluid with variable viscosity: Application of Adomian decomposition method. Commun Nonlinear Sci Numer Simulat, 14, 3844-3855.

Oahimire, J.I. and Olajuwon, B. I. (2014). Effects of radiation absorption and thermo-diffusion on MHD heat and mass transfer flow of a micro-polar fluid in the presence of heat Source, Applications and Applied mathematics, 9(2), 763-779.

Radhakrishnamacharya, G. and Srinisvasulu, Ch. (2007). Influence of wall properties on peristaltic transport with heat transfer. CR Mecanique, 335, 369-373.

Ramachandra, R.A. and Usha, S. (1995). Peristaltic Transport of Two Immiscible Viscous Fluids in a Circular Tube. Journal of Fluid Mechanics, 298, 271-285.

Ravikumar, S. (2013). Hydromagnetic peristaltic flow of blood with effect of porous medium through coaxial vertical channel: A Theoretical Study. International Journal of Engineering Sciences &Research Technology, 2(10), 2863-2871.

Ravikumar, S. (2013). Peristaltic fluid flow through magnetic field at low Reynolds number in a flexible channel under an oscillatory flux. International journal of Mathematical Archive, 4(1), 36-52.

Ravikumar, S. (2013). Peristaltic transportation with effect of magnetic field in a flexible channel under an oscillatory flux. Journal of Global Research in Mathematical Archives, 1(5), 53-62.

Ravikumar, S. (2014). Peristaltic flow of blood through coaxial vertical channel with effect of magnetic field: Blood flow study. International Journal of Recent advances in Mechanical Engineering (IJMECH), 3(4), 85-96.

Ravikumar, S. (2015). Effect of couple stress fluid flow on magnetohydrodynamic peristaltic blood flow with porous medium trough inclined channel in the presence of slip effect-Blood flow study. International Journal of Bio-Science and Bio-Technology, 7(5), 65-84.

Ravikumar, S. (2015). Effects of the couple stress fluid flow on the magnetohydrodynamic peristaltic motion with a uniform porous medium in the presence of slip effect. Jordan Journal of Mechanical and Industrial Engineering (JJMIE), 9(4), 269 – 278.

Ravikumar, S. and Siva Prasad, R. (2010). Interaction of pulsatile flow on the peristalticmotion of couple stress fluid through porous medium in a flexible channel. Eur. J. Pure Appl. Math, 3, 213-226.

Ravikumar, S., Prabhakara Rao, G. and Siva Prasad, R. (2010). Peristaltic flow of a second order fluid in a flexible channel. Int. J. of Appl. Math and Mech., 6 (18), 13-32.

Ravikumar, S., Prabhakara Rao, G. and Siva Prasad, R. (2010). Peristaltic flow of a couple stress fluid flows in a flexible channel under an oscillatory flux. Int. J. of Appl. Math and Mech., 6(13), 13 58-71.

Sanjib Sengupta (2015). Free Convective Chemically Absorption Fluid Past an Impulsively Accelerated Plate with Thermal Radiation Variable Wall Temperature and Concentrations. Applications and Applied mathematics, 10 (1), 328 – 348.

Seddeek, M. A. and Almushigeh, A. A. (2010). Effects of radiation and variable viscosity on MHD free convective flow and mass transfer over a stretching sheet with chemical reaction. Applications and Applied mathematics, 5 (1), 181-7197.

Shapiro, A.M., Jaffrin, M.Y. and Weinberg, S. L. (1969). Peristaltic pumping with long wave Lengths at Low Reynolds Number. J. Fluid Mechanics, 37, 799-825.

Siddiqui, A.M. and Schwarz, W.H. (1994). Peristaltic flow of a second order fluid in tubes. Journal of Non- Newtonian Fluid Mechanics, 35, 257-284.

Sobh, A.M. (2004). Peristaltic transport of a Magneto- Newtonian fluid through a porous medium. J. of the Islamic University of Gaza, 12, 37- 49.

Sohail Nadeem and Safia Akram (2011). Magnetohydrodynamic peristaltic flow of a hyperbolic tangent fluid in a vertical asymmetric channel with heat transfer. Acta Mech. Sin., 27(2), 237-250.

Srinivas, S. and Kothandapani, M. (2008). Peristaltic transport in an asymmetric channel with heat transfer - A note. International Communications in Heat and Mass Transfer, 35, 514-522.

Srivastava, L.M. (1986). Peristaltic transport of a couple stress fluid. Rheological Acta, 25,638-641.

Srivastava, L.M. and Srivastava, V.P. (1988). Peristaltic Transport of a Power-Law Fluid: Application to the Ductus Efferentes of the Reproductive Tract. Rheological Acta, 27, 428-433.

Srivastava, L.M., and Srivastava, V.P. (1984). Peristaltic Transport of Blood: Casson Model-II. J. Biomechanics, 17, 821-829.

Srivastava, L.M., Srivastava, V.P. and Sinha S.N. (1983). Peristaltic Transport of a Physiological Fluid, 1. Flow in Non-Uniform Geometry. Biorheology, 20, 153-166.

Takabatake, S. and Ayukawa, K. (1982). Numerical Study of Two Dimensional Peristaltic Flows. Journal of Fluid Mechanics, 122, 439-465.

Takabatake, S. and Ayukawa, K. (1988). Peristaltic Pumping in Circular Cylindrical Tubes: A Numerical Study of Fluid Transport and its Efficiency. Journal of Fluid Mechanics, 193, 267-283.

Vajravelu, K., Sreenadh, S. and Lakshminarayana, P. (2011). The influence of heat transfer on peristaltic transport of a Jeffrey fluid in a vertical porous stratum. Commun Nonlinear Sci Numer Simulat, 16, 3107-3125.